Intramolecular Activation of Aliphatic Carbon-Hydrogen Bonds at Tantalum(V) Metal Centers: A Comparison of Activation by Methyl and Methylidene Functional Groups

Linda R. Chamberlain,[†] Ian P. Rothwell,*[†] and John C. Huffman[‡]

Contribution from the Department of Chemistry, Purdue University, West Lafayette, Indiana 47907, and the Molecular Structure Center, Indiana University, Bloomington, Indiana 47405. *Received July 10, 1985*

Abstract: The compounds $Ta(OAr')_2(CH_3)_3$ and $Ta(OAr'\text{-}OMe)_2(CH_3)_3$ containing the sterically demanding aryloxide ligands 2,6-di-*tert*-butylphenoxide (OAr') and 2,6-di-*tert*-butyl-4-methoxyphenoxide (OAr'-OMe) have been isolated and both their thermal and photochemical reactivity investigated. On thermolysis both compounds undergo cyclometalation of one of the *tert*-butyl groups of each aryloxide ligand, with the elimination of 2 equiv of methane. In contrast, photolysis effects a clean conversion to a methylidene complex, $Ta(OAr')_2(=CH_2)(CH_3)$, and methane. On standing the methylidene compound converts to a monocyclometalated compound by intramolecular addition of a carbon-hydrogen bond of a *t*-Bu group to the tantalum-carbon double bond. Labeling studies clearly show that the methylidene complex is not thermally accessible. Kinetic studies of the two thermal cyclometalations of $Ta(OAr')_2(CH_3)_3$ show the reactions to be first order with a slightly negative entropy of activation. In contrast, kinetic data indicate that the intramolecular addition to the $Ta{=}CH_2$ function is severely entropically inhibited ($\Delta S^{\ddagger} = -30 \pm 6$ eu) although enthalpically favored over activation by $Ta\text{-}CH_3$ groups. The mechanistic implications of these results are discussed. Single-crystal X-ray diffraction studies on both trimethyl complexes show essentially identical structures containing an approximately TBP geometry about the tantalum atom, with axial aryloxide ligands. The steric congestion caused by the aryloxide *tert*-butyl groups results in a number of distortions to the coordination geometry. Crystal data for $Ta(OAr')_2(CH_3)_3$ at −165 °C are the following: $a = 17.797$ (4) Å, $b = 6.587$ (1) Å, $c = 23.253$ (5) Å, $\beta = 96.11$ (1)°, $Z = 4$, $d_{calcd} = 1.403$ g cm^{-3} in space group $C2$ of the 2173 unique intensities collected with Mo Kα, the 1995 with $F_o > 2.33\sigma(F)$ were used in the least-squares refinement to give residual $R(F) = 0.026$, $Rw(F) = 0.025$. Crystal data for $Ta(OAr'\text{-}OMe)_2(CH_3)_3$ at −159 °C are the following: $a = 14.385$ (4) Å, $b = 25.343$ (10) Å, $c = 9.980$ (2) Å, $Z = 4$, $d_{calcd} = 1.414$ g cm^{-3} in space group *Pnma*. Using the 2545 unique intensities with $F_o > 3.00\sigma(F)$ yielded final residuals $R(F) = 0.034$ and $Rw(F) = 0.035$.

Over the last few years the high-valent early d-block, lanthanide and actinide metal to carbon σ-bond (metal alkyl) has been shown to be capable of activating aliphatic carbon-hydrogen bonds both inter- and intramolecularly.[1-5] Hence a relatively new type of hydrocarbon activation has been characterized in which the previously well documented oxidative-addition activation pathway cannot take place.[6] The high valent, early transition metal to carbon double bond (metal alkylidene) has been shown to be an important functional group in a number of catalytic and stoichiometric organometallic reactions,[7] particularly olefin metathesis,[8] Wittig-type functionalizations of ketones and imines,[9] hydrogenation to alkane, and formation of ketenes by insertion of carbon monoxide.[10] We recently communicated our preliminary findings indicating the potential of metal-alkylidenes for carbon-hydrogen bond activation.[11] We report here a more thorough synthetic and mechanistic investigation of the activity of tantalum-methylidene ($Ta{=}CH_2$) groups for intramolecular aliphatic C-H bond activation (in particular those of 2,6-di-*tert*-butylphenoxide) and a comparison of their potency for the reaction with their "saturated" functional counterparts, tantalum-methyl ($Ta\text{-}CH_3$) groups.

Results and Discussion

Synthesis and Characterization. Treatment of $TaCl_5$ with an excess of the lithium aryloxides LiOAr' and LiOAr'-OMe (OAr' = 2,6-di-*tert*-butylphenoxide; OAr'-OMe = 2,6-di-*tert*-butyl-4-methoxyphenoxide) in hydrocarbon solvents yields the bis-substituted complexes $Ta(OAr')_2Cl_3$ (**1a**) and $Ta(OAr'\text{-}OMe)_2Cl_3$ (**1b**), respectively. Orange **1a** has been reported previously and shown to be mononuclear in the solid state, adopting a structure best represented as a square-pyramidal coordination about tantalum with one axial and one basal aryloxide ligand.[12] Red **1b** has been isolated by similar techniques and presumably adopts a similar structure. Treatment of **1** with a suspension of methyllithium in benzene results in the rapid replacement of the three halide ligands and formation of colorless solutions of $Ta(OAr')_2(CH_3)_3$ (**2a**) and $Ta(OAr'\text{-}OMe)_2(CH_3)_3$ (**2b**) (Scheme I). Filtration to remove LiCl and excess $LiCH_3$ followed by

Scheme I

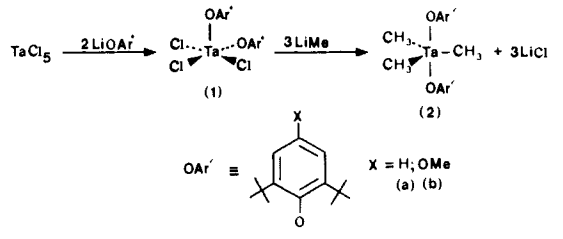

[†] Purdue University.
[‡] Indiana University.

(1) Rothwell, I. P. *Polyhedron* **1985**, *4*, 177.
(2) (a) Bennett, C. R.; Bradley, D. C. *J. Chem. Soc., Chem. Commun.* **1974**, 29. (b) Simpson, S. J.; Anderson, R. A. *Inorg. Chem.* **1981**, *20*, 3627. (c) Simpson, S. J.; Turner, H. W.; Andersen, R. A. *Inorg. Chem.* **1981**, *20*, 2991. (d) Planalp, R. P.; Andersen, R. A.; Zalkin, A. *Organometallics* **1983**, *2*, 16. (e) Planalp, R. P.; Andersen, R. A. *Organometallics* **1983**, *2*, 1675. (f) Nugent, W. A.; Overall, D. W.; Holmes, S. J. *Organometallics* **1983**, *2*, 161.
(3) (a) Bercaw, J. E. *Pure* Appl. *Chem.* **1984**, *56*, 1. (b) Mayer, J. M.; Curtis, C. J.; Bercaw, J. E. *J. Am. Chem. Soc.* **1983**, *105*, 2651.
(4) (a) Fredrick, C. M.; Marks, T. J. *J. Am. Chem. Soc.* **1984**, *106*, 2214. (b) Bruno, J. W.; Marks, T. J.; Day, V. W. *J. Am. Chem. Soc.* **1982**, *104*, 7357.
(5) (a) Watson, P. L.; Parshall, G. W. *Acc. Chem. Res.* **1985**, 51. (b) Watson, P. L. *J. Am. Chem. Soc.* **1983**, *105*, 6491. (c) Watson, P. L. *J. Chem. Soc., Chem. Commun.* **1983**, 276. (d) Watson, P. L. *J. Am. Chem. Soc.* **1982**, *104*, 337.
(6) (a) Shilov, A. E. "Activation of Saturated Hydrocarbons by Transition Metal Complexes"; Kluwer Academic, 1984. (b) Parshall, G. W. *Catalysis* **1977**, *1*, 335. (c) Webster, D. E. *Adv. Organomet. Chem.* **1977**, *15*, 147. (d) Shilov, A. E.; Shteinman, A. A. *Coord. Chem. Rev.* **1977**, *24*, 97. (e) Bruce, M. I. *Angew. Chem., Int. Ed. Engl.* **1977**, *16*, 73. (f) Dehand, J.; Pfeffer, M. N. *Coord. Chem. Rev.* **1976**, *18*, 327. (g) Parshall, G. W. *Acc. Chem. Res.* **1975**, *8*, 113; **1970**, *3*, 139. (h) Green, M. L. H. *Pure Appl. Chem.* **1978**, *50*, 27. (i) Parshall, G. W. "Homogeneous Catalysis"; John Wiley and Sons: New York, 1980. (j) Janowicz, A. H.; Bergman, R. G. *J. Am. Chem. Soc.* **1983**, *105*, 3929. (k) Jones, W. D.; Feher, F. J. *Organometallics* **1983**, *2*, 2563. (l) Hoyano, J. K.; Graham, W. A. G. *J. Am. Chem. Soc.* **1982**, *104*, 3723.
(7) (a) Schrock, R. R. In "Inorganic Chemistry Toward the 21st Century"; American Chemical Society Symposium Series, Chisholm, M. H., Ed. (b) Schrock, R. R. *Acc. Chem. Res.* **1979**, *12*, 98. (c) Grubbs, R. H. *Prog. Inorg. Chem.* **1978**, *24*, 1.

0002-7863/86/1508-1502$01.50/0

Table I. Crystallographic Data for $Ta(OAr')_2Me_3$(*2a*) and $Ta(OAr'OMe)_2Me_3$(*2b*)

	2a	**2b**
formula	$TaC_{31}H_{51}O_2$	$TaC_{33}H_{55}O_4$
fw	636.69	696.74
space group	*C*2	*Pnma*
a, Å	17.797 (4)	14.385 (4)
b, Å	6.587 (1)	25.343 (10)
c, Å	23.253 (5)	9.980 (2)
β, deg	96.11 (1)	
Z	4	4
V, Å^3	3015.1	3273.8
density (calcd), g/cm^3	1.403	1.414
crystal size, mm	*a*	0.12 × 0.12 × 0.18
crystal color	colorless	yellow
radiation	Mo Kα (λ = 0.71069 Å)	Mo Kα (λ = 0.71069 Å)
linear abs coeff, cm^{-1}	36.244	33.483
temp, °C	−165	−159
detector aperture	3.0 mm wide × 4.0 mm 22.5 cm from crystal	3.0 mm wide × 4.0 mm high 22.5 cm from crystal
sample to source distance, cm	23.5	23.5
takeoff angle, deg	2.0	2.0
scan speed, deg/min	4.0	4.0
scan width, deg	2.0 + 0.692 tan θ	2.0 + 0.692 tan θ
background counts, s	3	8
2θ range, deg	6–45	6–50
data collected	4334	3360
unique data	2173	2908
unique data with $F_o > 2.33\sigma(F)$	1995	2545[b]
R(*F*)	0.0258	0.0340
Rw(*F*)	0.0245	0.0354
goodness of fit	0.683	0.895
largest δ/σ	0.05	0.05

[a] Crystal dimensions were the following: face = 1 0 0, *d* = 0.0500 mm; face = −1 0 0, *d* = 0.0500 mm; face = 0 0 1, *d* = 0.1000 mm; face = 0 0 −1, *d* = 0.1000 mm; face = 0 1 0, *d* = 0.1200 mm; face = 0 −1 0, *d* = 0.1200 mm. [b] $F_o > 3.00\sigma(F)$.

removal of solvents gives solid samples of **2**. If solutions of **2** are left in contact with the suspended $LiCH_3$ then the mixture becomes dark over a period of hours with the apparent evolution of methane gas. Presumably further alkylation by substitution of the two aryloxide ligands leads to the known, thermally unstable $TaMe_5$. Recrystallization of **2a,b** from cold hexane yields very pale-yellow crystals and both complexes have been subjected to a single-crystal X-ray diffraction study.

Solid-State Structures of $Ta(OAr')_2(CH_3)_3$ (2a) and $Ta(OAr'–OMe)_2(CH_3)_3$ (2b). Table I gives the crystallographic data for the two complexes while Tables II and III give the fractional coordinates and isotropic thermal parameters. Some important bond distances and angles are collected in Table IV. Figures 1 and 2 give two Ortep views of the complexes with the atom numbering scheme used. It can be seen that the two structures are very similar with the coordination about the metal best described as trigonal bipyramidal with the two aryloxide ligands being axial. However, there are some interesting distortions to the coordination geometry due to the large steric demand of the aryloxide ligands. The Ta–O distances of 1.930 (6) and 1.945 (6) Å (**2a**) and 1.925 (4) Å (**2b**) are shorter than expected for a single bond distance consistent with significant oxygen-p to tantalum-d π-bonding. The large Ta–O–C angles are also consistent with this, although they are very characteristic of early transition metal aryloxides in general.[13,14] It is interesting to note that the 4-methoxy substituent in **2b** has a negligible effect on the Ta–O distance. The π-electron releasing capabilities of this group would be expected to enhance the π-donor abilities of the OAr'-OMe ligand. In the complex Zr(OAr')(OAr'-OMe)-

Table II. Fractional Coordinates and Isotropic Thermal Parameters for $Ta(OAr')_2(CH_3)_3$ (**2a**)

atom	10^4x	10^4y	10^4z	$10B_{iso}$
Ta(1)	2504.1 (1)	749	2637.0 (1)	10
C(2)	2522 (5)	4005 (14)	2354 (4)	13
C(3)	3355 (5)	−1110 (17)	2890 (4)	21
C(4)	1643 (5)	−1134 (17)	2704 (5)	19
O(5)	2525 (3)	312 (8)	1817 (2)	11
C(6)	2531 (4)	1258 (12)	1278 (3)	16
C(7)	1913 (5)	1762 (16)	951 (4)	16
C(8)	1956 (6)	3064 (18)	486 (4)	25
C(9)	2558 (5)	3705 (19)	323 (4)	23
C(10)	3151 (5)	2964 (18)	595 (4)	23
C(11)	3167 (5)	1650 (16)	1067 (4)	18
C(12)	3842 (4)	694 (31)	1316 (3)	19
C(13)	4394 (4)	932 (37)	903 (4)	27
C(14)	3738 (5)	−1634 (19)	1383 (5)	23
C(15)	4130 (5)	1690 (20)	1885 (5)	27
C(16)	1223 (14)	923 (30)	1068 (3)	19
C(17)	679 (5)	1152 (22)	545 (4)	28
C(18)	1300 (5)	−1489 (19)	1128 (5)	24
C(19)	940 (5)	1797 (20)	1590 (4)	24
O(20)	2475 (3)	1977 (9)	3392 (2)	9
C(21)	2462 (4)	3556 (16)	3775 (4)	18
C(22)	1818 (4)	4384 (14)	3900 (4)	11
C(23)	1841 (4)	6150 (13)	4239 (3)	13
C(24)	2436 (5)	7024 (16)	4468 (4)	18
C(25)	3041 (4)	6146 (13)	4375 (3)	13
C(26)	3077 (5)	4369 (15)	4046 (4)	14
C(27)	3773 (4)	3374 (16)	4014 (4)	14
C(28)	3735 (4)	1153 (16)	4202 (4)	18
C(29)	3992 (5)	3584 (17)	3398 (4)	18
C(30)	4336 (5)	4326 (19)	4431 (4)	23
C(31)	1136 (4)	3356 (16)	3714 (4)	15
C(32)	550 (5)	4372 (18)	3980 (5)	22
C(33)	1164 (5)	1145 (16)	3895 (4)	20
C(34)	968 (5)	3565 (18)	3041 (4)	20

Table III. Fractional Coordinates and Isotropic Thermal Parameters for $Ta(OAr'–OMe)_2(CH_3)_3$ (**2b**)

atom	10^4x	10^4y	10^4z	$10B_{iso}$
Ta(1)	3083.2 (2)	2500*	9772.0 (3)	11
C(2)	3072 (7)	2500*	7357 (9)	20
C(3)	1873 (6)	2500*	11304 (9)	14
C(4)	4548 (6)	2500*	10249 (10)	16
O(5)	2969 (2)	3255 (1)	9927 (4)	12
C(6)	2572 (4)	3712 (2)	10485 (6)	14
C(7)	1837 (3)	3961 (2)	9679 (6)	13
C(8)	1400 (3)	4393 (2)	10341 (6)	14
C(9)	1652 (3)	4576 (2)	11723 (6)	14
C(10)	2425 (3)	4361 (2)	12450 (6)	13
C(11)	2909 (4)	3933 (2)	11820 (6)	13
C(12)	1533 (4)	3796 (2)	8093 (6)	16
C(13)	813 (5)	4177 (3)	7432 (7)	22
C(14)	1064 (5)	3251 (3)	8106 (7)	21
C(15)	2379 (4)	3816 (3)	7026 (7)	18
O(16)	1123 (3)	4980 (2)	12287 (4)	17
C(17)	1241 (4)	5100 (3)	13830 (7)	19
C(18)	3810 (4)	3752 (2)	12607 (6)	15
C(19)	3696 (4)	3201 (2)	13263 (7)	16
C(20)	4076 (4)	4111 (2)	13917 (7)	16
C(21)	4626 (4)	3781 (3)	11508 (7)	18

(8) Grubbs, R. H. "Comprehensive Organometallic Chemistry"; Wilkinson, G., Stone, F. G. A., Abel, E. V., Eds.; Pergamon Press: Oxford, 1982; Chapter 54.
(9) Rocklage, S.; Schrock, R. R. *J. Am. Chem. Soc.* **1980**, *102*, 7808.
(10) Mackenzie, P. B.; Ott, K. C.; Grubbs, R. H. *Pure Appl. Chem.* **1984**, *56*, 59.
(11) (a) Chamberlain, L. R.; Rothwell, A. P.; Rothwell, I. P. *J. Am. Chem. Soc.* **1984**, *106*, 1847. (b) Chamberlain, L. R.; Rothwell, I. P.; Huffman, J. C. *J. Am. Chem. Soc.* **1982**, *104*, 7338.
(12) Chamberlain, L. R.; Huffman, J. C.; Rothwell, I. P. *Inorg. Chem.* **1984**, *23*, 2575.
(13) Coffindaffer, T. W.; Rothwell, I. P.; Huffman, J. C. *Inorg. Chem.* **1983**, *22*, 2906.
(14) Latesky, S. L.; McMullen, A. K.; Niccolai, G. P.; Rothwell, I. P.; Huffman, J. C. *Organometallics* **1985**, *4*, 902.

Table IV. Selected Bond Distances (Å) and Angles (deg) for $Ta(OAr')_2(CH_3)_3$ (**2a**) and $Ta(OAr'-OMe)_2(CH_3)_3$ (**2b**)

	2a	2b
Ta–O(5)	1.930 (6)	1.925 (4)
Ta–O(20)	1.945 (6)	
Ta–C(2)	2.248 (10)	2.219 (8)
Ta–C(3)	2.136 (10)	2.169 (8)
Ta–C(4)	2.138 (10)	2.150 (8)

2a		2b	
O(5)–Ta–O(20)	164.1 (2)	O(5)–Ta–O(5)	167.2 (2)
O(5)–Ta–C(2)	81.1 (3)	O(5)–Ta–C(2)	83.6 (1)
O(5)–Ta–C(3)	95.2 (3)	O(5)–Ta–C(3)	94.1 (1)
O(5)–Ta–C(4)	95.2 (3)	O(5)–Ta–C(4)	94.0 (1)
O(20)–Ta–C(2)	83.0 (3)		
O(20)–Ta–C(3)	95.0 (3)		
O(20)–Ta–C(4)	94.1 (3)		
C(2)–Ta–C(3)	127.0 (4)	C(2)–Ta–C(3)	127.9 (3)
C(2)–Ta–C(4)	128.3 (4)	C(2)–Ta–C(4)	130.2 (3)
C(3)–Ta–C(4)	104.7 (4)	C(3)–Ta–C(4)	101.9 (4)
Ta–O(5)–C(6)	144.8 (5)	Ta–O(5)–C(6)	153.2 (3)
Ta–O(20)–C(21)	155.3 (6)		

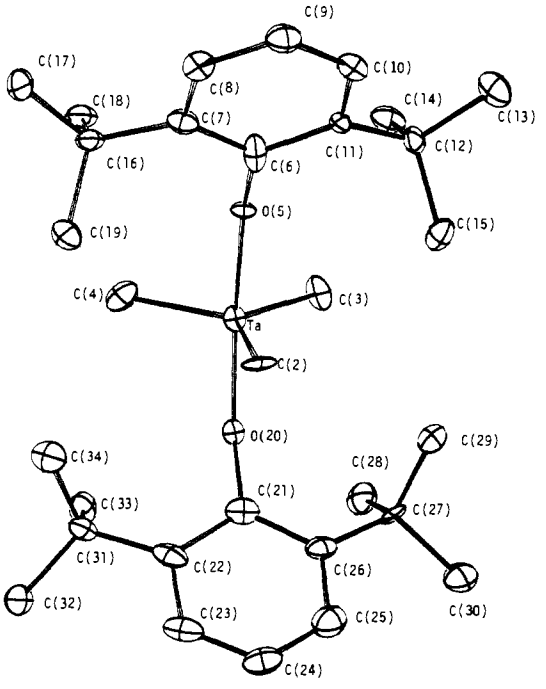

Figure 1. Ortep view and numbering scheme of $Ta(OAr')_2(CH_3)_3$ (**2a**).

$(CH_2Ph)_2$ the Zr–OAr'–OMe distance was found to be 0.03 Å shorter than the Zr–OAr' distance,[14] but in complexes **2a,b** the effect is much smaller. It can be seen from Figures 1 and 2 that the aromatic rings of the aryloxides are arranged so as to give virtual C_{2v} symmetry to **2a** and in fact crystallographic C_s symmetry to **2b** with the plane of symmetry containing the metal and three methyl groups. This conformation of the aryloxide results in one of the methyl groups, C(2), being significantly different than the remaining two. Furthermore, the two aryloxide oxygens are tilted toward this unique methyl group with an O–Ta–O angle of 164.1 (2)° and 167.2 (2)° for **2a** and **2b**, respectively. This movement from linearity of the two axial oxygen atoms represents an attempt to try to relieve the unfavorable steric interactions between the four sterically demanding *t*-Bu substituents and the two methyl groups C(3) and C(4). This effect is best illustrated by space-filling diagrams shown in Figure 3. Besides the bending of the aryloxide oxygens, this steric congestion also leads to a contraction of the C(3)–Ta–C(4) angle to 104.7 (4)° and 101.9 (4)° from the 120° expected for a regular TBP geometry. The most dramatic effect of these distortions is seen in the significant elongation that occurs of the Ta–C(2) bond by 0.11 Å in **2a** and

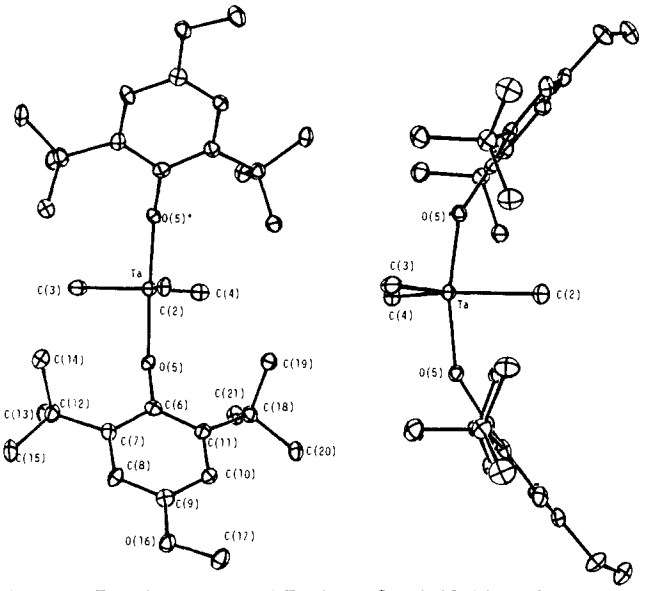

Figure 2. Two Ortep views of $Ta(OAr'-OMe)_2(CH_3)_3$ and the numbering scheme used.

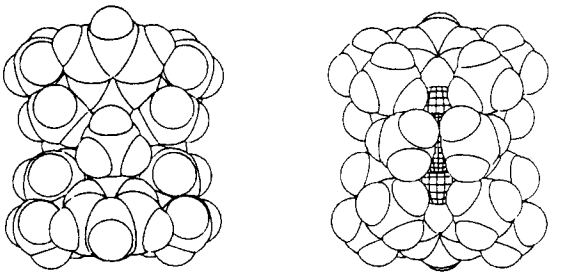

Figure 3. Two space-filling diagrams of $Ta(OAr')_2(CH_3)_3$: (A) looking down the C(2)–Ta bond; (B) looking between the C(3)–Ta–C(4) bonds.

0.05–0.06 Å in **2b** compared to the distances to C(3) and C(4). The cause of this elongation may either be steric, related to the four *tert*-butyl groups which "surround" the Ta–C(2) bond, or else electronic, due to the increased σ-bonding competition of the other methyl groups that are being pushed toward a position trans to this methyl group. It is interesting that in the sterically noncrowded complex $Ta(OAr)_2(CH_2Ph)_3$ (OAr = 2,6-dimethylphenoxide) although again a tbp geometry with axial oxygens is given, the oxygen atoms bend away from a unique carbon, opening up the angle between the two other benzyl groups to 127.8 (3)°. In this case the unique Ta–C distance is significantly *shorter* than that to the other two carbon atoms.[15]

It is apparent from Figures 1 and 2 that the conformation adopted by the *tert*-butyl groups is such as to minimize the interaction between their methyl groups and the metal center. For both **2a** and **2b** the hydrogen atoms were refined. It was found that for each *t*-Bu group there was one hydrogen atom located at distances of between 2.8 and 3.0 Å from the metal center. Similar M–HC distances have been observed for a number of other complexes of 2,6-di-*tert*-butylphenoxide[12,14] but there is no evidence as yet for any positive electronic interaction in the ground state, a situation now well documented in the literature for other systems.[16,17] The change from square-pyramidal to TBP on going from $Ta(OAr')_2Cl_3$ to $Ta(OAr')_2Me_3$ has been discussed previously.[12]

(15) Chamberlain, L. R.; Huffman, J. C.; Rothwell, I. P., results to be published.
(16) Brookhart, M.; Green, M. L. H. *J. Organomet. Chem.* **1983**, *250*, 395 and references therein.
(17) Tilley, T. D.; Andersen, R. A.; Zalkin, A. *J. Am. Chem. Soc.* **1982**, *104*, 3725.

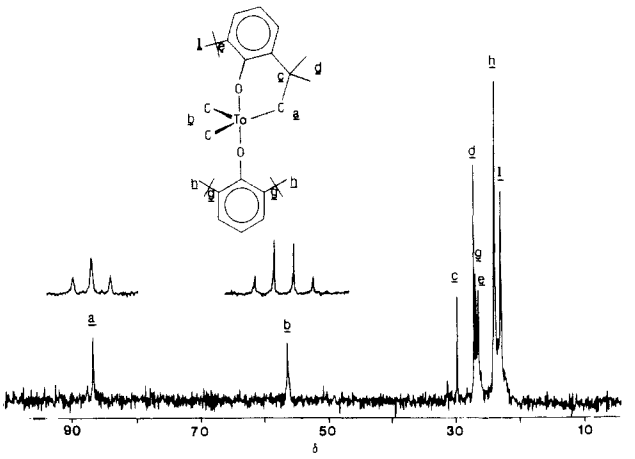

Figure 4. $[^1H]^{13}C$ NMR spectrum of $Ta(OC_6H_3\text{-}t\text{-}BuCMe_2CH_2)(OAr')(CH_3)_2$ (**3a**) between 0 and 100 ppm showing peak assignments. The ^1H coupled spectra of the cyclometalated $Ta\text{–}CH_2\text{–}CMe_3$ (a) and $Ta\text{–}CH_3$ (b) carbon atoms are shown.

Scheme II

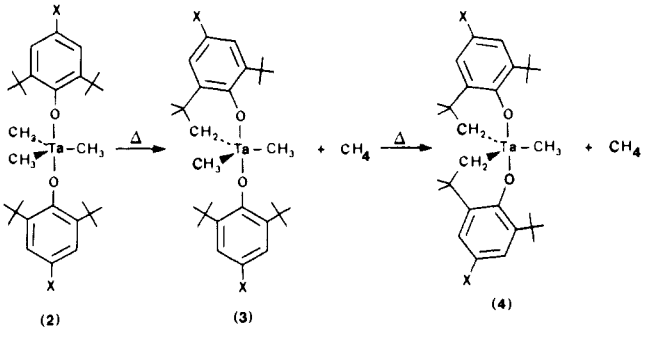

Thermal Reactivity. The thermolysis of the trimethyl complexes **2** in hydrocarbon solvents (typically toluene) leads to the elimination of first 1 and then 2 equiv of methane and the formation of the cyclometalated complexes **3** and **4** as shown (Scheme II). Relatively pure samples of the intermediate, monocyclometalated complex **3** can be obtained by thermolysis of **2** at 90 °C for 24 h, while **4** is generated at a significant rate only at temperatures above 100 °C. Both complexes are almost colorless and extremely soluble in all hydrocarbon solvents. The cyclometalation reaction involves the formation of a six-membered chelate ring by the activation of a carbon–hydrogen bond of one of the *tert*-butyl groups of each aryloxide, the hydrogen atom being lost with one of the tantalum–methyl groups as methane. Although the solid-state structures of **3** and **4** have not been determined, we have assigned them both structures based on a TBP geometry about tantalum with axial oxygen atoms (Scheme II). This has precedence for complex **3** in the known structure of the related monocyclometalated diphenyl complex $Ta(OC_6H_3\text{-}t\text{-}BuCMe_2CH_2)(OAr')(Ph)_2$[18] while for **4** spectroscopic data are consistent (but not conclusive) with this type of structure. Both metalated complexes exhibit resonances in their ^1H and ^{13}C NMR spectra characteristic of the six-membered metallacycle. In the dimethyl complex **3**, besides peaks due to the nonmetalated *t*-Bu groups, the new $Ta\text{–}CH_2CMe_3$ function is indicated in the ^1H NMR by two singlets in the ratio of 2:6 at δ 2.07 and δ 1.20 while the Ta–C(chelate) carbon resonates at δ 94.6 in the ^{13}C NMR spectrum. This peak is 30 ppm more downfield than the $Ta(CH_3)_2$ groups in this complex (Figure 4). This downfield shifting of the carbon atoms contained in cyclometalated rings has been noted before,[19] and similar shifts were seen for 2,6-di-*tert*-butylphenoxide cyclometalated by titanium and zirconium.[20] In the bis-cyclometalated complex **4a** the $Ta\text{–}CH_2CMe_2$–carbon is again evident downfield at δ 95.6, but the ^1H NMR spectrum now shows the $Ta\text{–}CH_2CMe_2$ protons as an AB pattern and two singlets, respectively. This is to be expected from a structure in which equivalent chelate rings are not contained on a mirror plane, the methylene protons and methyl groups hence becoming diastereotopic. There appears to be four possible isomers based on either a TBP or square-pyramidal geometry that would be consistent with these data, but for convenience we will represent **4** only by the isomer shown in Scheme II.

Scheme III

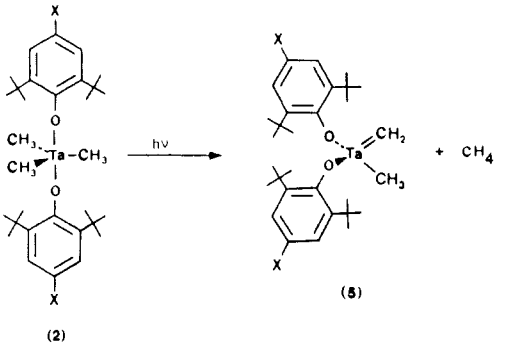

Scheme IV

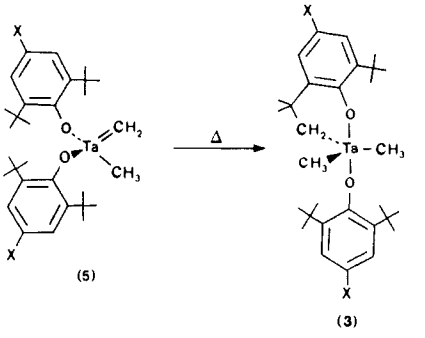

Photochemical Reactivity. On photolysis in hydrocarbon solvents with an ultraviolet light source, the trimethyl complexes **2** lose 1 equiv of methane and form essentially quantitative yields of the methylidene complexes $Ta(OAr')_2(=CH_2)(CH_3)$ (**5a**) and $Ta(OAr'\text{–}OMe)_2(=CH_2)(CH_3)$ (**5b**) (Scheme III). This reaction is readily monitored by ^1H NMR. Hence, the two aliphatic peaks at δ 1.19 (s, $Ta\text{–}CH_3$) and δ 1.45 (s, *t-Bu*) in the spectrum of **2a** are replaced on photolysis in C_6D_6 by three peaks at δ 1.20 (s, $Ta\text{–}CH_3$), δ 1.50 (s, *t-Bu*), and δ 9.41 (s, $Ta{=}CH_2$) in the ratio of 3:36:2. Methane is also shown by a peak at δ 0.2. Besides the characteristic resonance in the ^1H NMR, the methylidene function is also confirmed by a peak in the ^{13}C NMR at δ 236.2 for **5a** and 234.6 ppm for **5b** as well as the reaction of **5** with acetone to generate isobutylene. Hence, complex **5** represents an example of an early transition-metal methylidene complex, a functional group having well documented reactivity in a number of important stoichiometric organometallic transformations.[21] Although the structure of the methyl, methylidene complex is unknown we believe it to be similar to the structurally characterized alkylidene complex $Ta(OAr')_2(=CHSiMe_3)(CH_2SiMe_3)$.[11] Attempts to isolate the photogenerated methylidene complex were thwarted by its high thermal reactivity. Over a period of hours at room temperature solutions of the methylidene convert to the mono-

(18) Chamberlain, L. R.; Keddington, J.; Huffman, J. C.; Rothwell, I. P. *Organometallics* **1982**, *1*, 1538.
(19) Deeming, A. J.; Rothwell, I. P. *Pure Appl. Chem.* **1980**, *52*, 649 and references therein.
(20) Latesky, S. L.; McMullen, A. K.; Rothwell, I. P.; Huffman, J. C. *J. Am. Chem. Soc.*, in press.
(21) (a) Schrock, R. R.; Sharp, P. R. *J. Am. Chem. Soc.* **1978**, *100*, 2389. (b) Buchwald, S. L.; Cannizzo, L.; Clawson, L.; Ho, S.; Meinhart, D.; Stille, J. R.; Straus, D.; Grubbs, R. H. *Pure Appl. Chem.* **1983**, *55*, 1733. (c) Ott, K. C.; Grubbs, R. H. *J. Am. Chem. Soc.* **1981**, *103*, 5922. (d) Holmes, S. J.; Schrock, R. R. *J. Am. Chem. Soc.* **1981**, *103*, 4599. (e) Hayes, J. C.; Cooper, N. J. *J. Am. Chem. Soc.* **1982**, *104*, 5570. (f) Hayes, J. C.; Pearson, G. D. N.; Cooper, N. J. *J. Am. Chem. Soc.* **1981**, *103*, 4648.

Scheme V

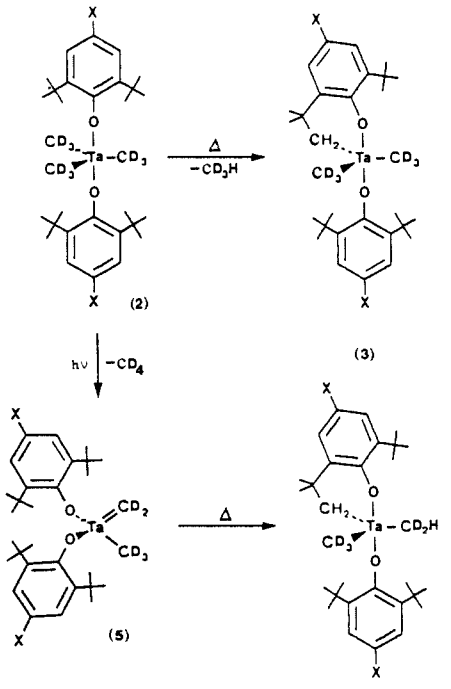

cyclometalated complex **3**. This "isomerization" involves the intramolecular addition of one of the C–H bonds of an aryloxide *tert*-butyl group across the tantalum–carbon double bond, converting the methylidene group back to a methyl group (Scheme IV). This step can be thought of as an intramolecular reverse of the α-hydrogen abstraction process. A more thorough analysis of the photochemical α-hydride abstraction process will be reported in a later paper.[22]

Labeling Studies and Kinetic Measurements. To gain more insight into the thermal and photochemical reactivity of the trimethyl complexes we have carried out a combination of labeling studies and kinetic measurements. The deuterated complex Ta(OAr')$_2$(CD$_3$)$_3$ (**2a**-d_9) is readily synthesized from the trichloride with LiCD$_3$. Mass spectrometric analysis of samples of this complex with use of either electron impact or chemical ionization methods[23] indicates an isotopic purity of 95% d_9 with <5% d_8, consistent with the quoted enrichment of the methyl iodide used (99.5% deuterated, Merck and Co.). Thermolysis of this complex yielded the monocyclometalated complex **3a** and CHD$_3$. Mass spectrometric analysis confirmed the product to be **3a**-d_6 with <4% of the d_5 complex. Further thermolysis yielded the bis-cyclometalated complex shown to be >98% **4a**-d_3. The ^{1}H and ^{13}C NMR spectra of these labeled complexes were identical with their unlabeled counterparts except for the lack of Ta–*Me* resonances in the ^{1}H NMR and the splitting of the Ta–*C*D$_3$ resonances into broad multiplets in the ^{13}C NMR spectrum. The photolysis and ensuing thermal reactivity of Ta(OAr')$_2$(CD$_3$)$_3$ can be followed by monitoring the change in the aryloxide signal. The final, monocyclometalated complex formed via the photogenerated methylidene was shown by mass spectrometric analysis to be **3a**-d_5 with <5% d_6 and <3% d_4 (Experimental Section). Careful analysis of the ^{1}H NMR spectrum of this complex at 470 MHz showed a weak multiplet at δ 1.05 which we assign to a Ta–CD$_2$*H* resonance. These results are consistent with the reactivity pathways outlined in Scheme V. The thermal elimination of methane involves the direct loss of one of the *tert*-butyl group hydrogen atoms with a Ta–CD$_3$ group to form a monocyclometalated complex with two Ta–CD$_3$ functions remaining. However, the photochemical pathway involves the initial formation of CD$_4$ by photochemical α-hydrogen abstraction to form a Ta=CD$_2$ group. The addition of a C–H bond of one of the aryloxide *t*-Bu groups then produces a monocyclometalated complex containing a Ta–CD$_2$H substituent. Hence, the methylidene complex **5a** is clearly not an intermediate in the thermal formation of the monocyclometalated complex directly from the trimethyl compound. The thermal intermediacy of a methylidene complex in the formation of (η^6-C$_5$Me$_4$CH$_2$)(η^5-C$_5$Me$_5$)TiCH$_3$ from (η^5-C$_5$Me$_5$)$_2$Ti(CH$_3$)$_2$ has been demonstrated by similar labeling studies.[24]

We have also used kinetic methods to study the three thermal steps that we have identified in which intramolecular aliphatic CH bond activation is taking place. By using ^{1}H NMR monitoring techniques we find that the two ring-closure reactions for form the mono- and bis-cyclometalated complexes from Ta(OAr')$_2$(CH$_3$)$_3$ (**2a**) follow first-order kinetic behavior over close to 4 half-lives. The reactions were monitored by observing both the disappearance of staring material peaks, either **2a** or **3a**, and the appearance of product peaks, either **3a** or **4a**, respectively, for the two reactions. The reactions were followed at a range of temperatures in order for activational parameters to be obtained. The rate-constant data obtained are given in Table V and shown graphically in Figure 5 as a plot of ln (k/T) vs. T^{-1} (K^{-1}). The

Table V. Rate Constants for Intramolecular Cyclometalation Reactions

Ta(OAr-)$_2$(CH$_3$e$_2$ (**2a**) → Ta(OC$_6$H$_3$-*t*-BuCMe$_2$CH$_2$)OAr-(CH$_3$)$_2$ (**3a**) + CH$_4$

T, °C	10^5k, s^{-1}
75	0.45 ± 0.05
91	3.10 ± 0.15
106	13.0 ± 1.5
128	78.0 ± 7.0

Ta(OC$_6$H$_3$-*t*-BuOMe$_2$CH$_2$)(OAr-)(CH$_3$)$_2$ (**3a**) → Ta(OC$_6$H$_3$-*t*-BuCMe$_2$CH$_2$)$_2$(CH$_3$) (**4a**) + CH$_4$

T, °C	10^5k, s^{-1}
106	0.42 ± 0.05
119	2.21 ± 0.20
128	2.91 ± 0.20
137	8.25 ± 0.70
151	35.4 ± 3.0

Ta(OAr--X)$_2$(=CH$_2$)(CH$_3$) (**5**) → Ta(OC$_6$H$_3$-*t*-BuXCMe$_2$CH$_2$)(OAr'—X)(CH$_3$)$_2$ (**3**)

X = H		X = OMe	
T, °C	10^5k, s^{-1}	T, °C	10^5k, s^{-1}
27	4.30 ± 0.3	28	3.75 ± 0.4
39	8.3 ± 0.8	38	10.2 ± 1.0
49	20.8 ± 2.0	48	20.2 ± 2.0
60	48.9 ± 4.2	57	40.3 ± 4.0

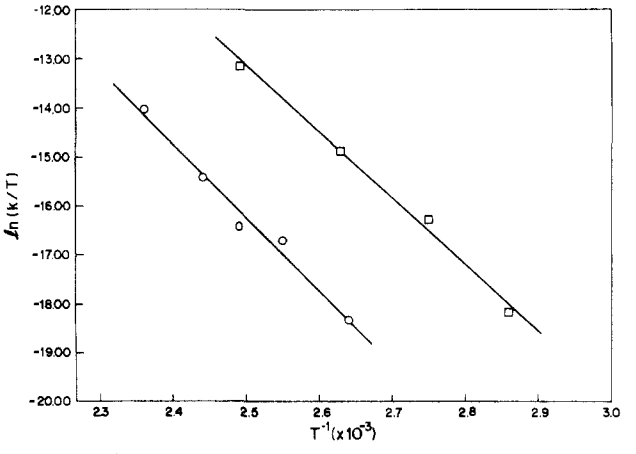

Figure 5. Activated complex theory plot for the first (□) and second (○) cyclometalation reactions of Ta(OAr')$_2$(CH$_3$)$_3$ depicted in Scheme II.

(22) Chamberlain, L. R.; Rothwell, I. P., results to be published.
(23) Rothwell, A. P.; Rothwell, I. P., results to be published.
(24) McDade, C.; Green, J. C.; Bercaw, J. E. *Organometallics* **1982**, *1*, 1629.

Table VI. Activation Parameters for Intramolecular Carbon–Hydrogen Bond Activation at d° and Related Metal Centers[a]

reaction	$\Delta H^{\ddagger}$, kcal mol^{-1}	$\Delta S^{\ddagger}$, eu
$Ta(OAr')_2(CH_3)_3 \rightarrow Ta(O\text{–}CH_2)(OAr')(CH_3)_2 + CH_4$	26.4 ± 1.0	−7 ± 3
$Ta(O\text{–}CH_2)(CH_3)_2 \rightarrow Ta(O\text{–}CH_2)_2(CH_3) + CH_4$	29.5 ± 1.0	−6 ± 3
$Ta(OAr')_2(CH_2)(CH_3) \rightarrow Ta(O\text{–}CH_2)(OAr')(CH_3)_2$	14.3 ± 1.02	−31 ± 6
$Ta(OAr'\text{–}OMe)_2(CH_2)(CH_3) \rightarrow Ta(O\text{–}CH_2)(OAr\text{–}OMe)(CH_3)_2$	15.4 ± 1.1	−28 ± 6
$Ti(OAr')_2(CH_2Ph)_2 \rightarrow Ti(O\text{–}CH_2)(OAr')(CH_2Ph) + CH_3Ph$	23.0 ± 1.0	−13 ± 3
$Zr(OAr')_2(CH_2Ph)_2 \rightarrow Zr(O\text{–}CH_2)(OAr')(CH_2Ph) + CH_3Ph$	21.6 ± 1.0	−19 ± 3
$Cp_2{}^*Th(CH_2CMe_3)_2 \rightarrow Cp_2{}^*Th(CH_2CMe_2CH_2) + CMe_4$	20.6 ± 0.6	−17 ± 2
$Cp_2{}^*Th(CH_2SiMe_3)_2 \rightarrow Cp_2{}^*Th(CH_2SiMe_2CH_2) + SiMe_4$	25.2 ± 0.9	−9 ± 1

[a] (O–CH_2) = cyclometalated 2,6-di-*tert*-butylphenoxide.

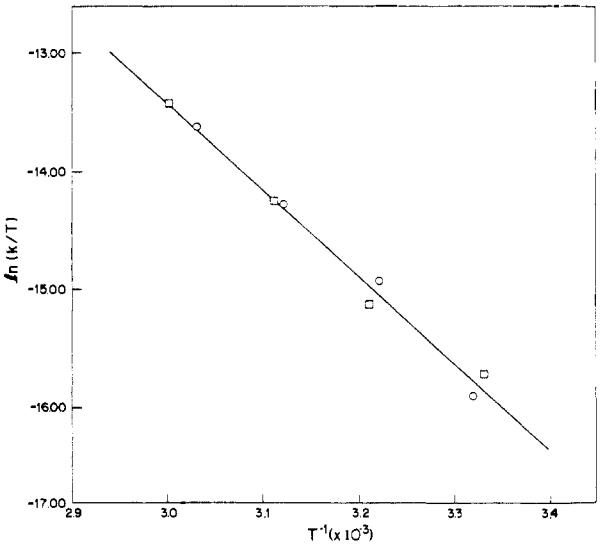

Figure 6. Activated complex theory plots for the intramolecular ring closure of $Ta(OAr')_2(=CH_2)(CH_3)$ (□) and $Ta(OAr'\text{–}OMe)_2(=CH_2)(CH_3)$ (○).

activation parameters are collected in Table VI. The rates of cyclometalation of the complex $Ta(OAr'\text{–}OMe)_2(CH_3)_3$ (**2b**) and the labeled complex $Ta(OAr')_2(CD_3)_3$ were found to be identical with that of $Ta(OAr')_2(CH_3)_3$ (**2a**) at 125 °C, and hence detailed kinetic measurements on these complexes were not made.

It was found possible to also follow the formation of the monometalated complex **3a** from the photogenerated intermediate methylidene complex **5a** by monitoring the disappearance of the distinctive $Ta{=}CH_2$ resonance over time. Again first-order kinetic behavior for the disappearance of the methylidene was observed. For this reaction it was also decided to carry out a kinetic analysis of the ring-closure reaction of the 4-methoxy complex, i.e., **5b–3b** for comparison. Plots of ln (k/T) vs. T^{-1} for these two reactions are shown in Figure 6. Although only one fitting line is shown, both sets of data were treated separately and the resulting activation parameters are collected in Table VI.

Mechanistic Interpretation. Although the number of systems studied kinetically that involve the intramolecular activation of CH bonds at d° and related metal centers is relatively small, a pattern has emerged in which the reactions are characterized by moderately large and negative entropies of activation. These data have been accommodated into a reaction mechanism involving a multicenter transition state in which the new metal–carbon bond is being formed simultaneous with the breaking of the metal-leaving group (typically alkyl) bond and transfer of the hydrogen atom. Similar types of transition states have been put forward for the hydrogenolysis of d° metal and lithium alkyls.[25,26] Both the labeling studies and kinetic data that we have obtained for the two thermal cyclometalation reactions of the trimethyl complex $Ta(OAr')_2(CH_3)_3$ (**2a**) are consistent with this picture of direct

Scheme VI

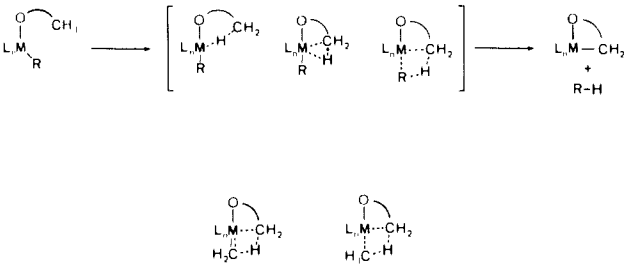

loss of methane via a four-center, four-electron transition state (Scheme VI). However, it can be seen that the entropies of activation are only slightly negative, and significantly less negative than those found for cyclometalation of the same ligand in the complexes $M(OAr')_2(CH_2Ph)_2$ (M = Ti, Zr) (Table VI).[20] The critical importance of steric effects on cyclometalation reactions has been recognized and elegantly demonstrated by Shaw and co-workers.[27] The presence of bulky substituents on the ligand to be metalated has been argued to favor the reaction by decreasing the loss in rotational entropy that occurs on chelation (cyclization). We believe the smaller negative entropy of activation for the cyclometalation of 2,6-di-*tert*-butylphenoxide at Ta(V) compared to Ti(IV) and Zr(IV) metal centers reflects the more steric demands of the five-coordinate coordination sphere. Hence, the more restricted mobility expected of the aryloxide *tert*-butyl groups in the tantalum complex would be expected to reduce the loss of rotational entropy on going to the more ordered transition state in which a particular C–H bond of a *t*-Bu group is being activated. The most significant difference between the first and second cyclometalation steps lies in the enthalpies of activation. Here the second cyclometalation is enthalpically inhibited over the first by 3 kcal mol^{-1}. Bearing in mind the elongation of one of the $Ta\text{–}CH_3$ bonds observed in the ground-state structures of the trimethyl complexes (vide supra) it is tempting to ascribe this enthalpic difference to an overall weakening of the $Ta\text{–}CH_3$ bonds in the trimethyl complex compared to the monocyclometalated, dimethyl product. Indeed, in the *mono*cyclometalated complex $Ta(OC_6H_3\text{-}t\text{-}BuCMe_2CH_2)(OAr')(Ph)_2$ the Ta–C distances are all similar. However, such an argument is clearly fraught with dangerous oversimplifications.

We turn now to the ring closure involving the methylidene complex. If one accepts the idea of a four-center, four-electron transition state for the elimination of alkane from these d° metal–alkyl systems, then it seems logical that metal–alkylidene functional groups would be enthalpically more potent for C–H bond activation. This can be shown by directly considering the two expected transition states (Scheme VI). In the case of alkane loss, one is both making and breaking metal–carbon σ-bonds with the concomitant hydrogen transfer. However, in adding a carbon–hydrogen bond across a $Ta{=}CH_2$ double bond one is gaining a metal–carbon σ-bond "only" at the expense of a metal–carbon π-bond. One emphasizes the "only" because hard data on the strength of the π-component of this $Ta\text{–}CH_2$ are not available. However, it seems reasonable that it should be considerably less,

(25) (a) Gell, K. I.; Schwartz, J. *J. Am. Chem. Soc.* **1978**, *100*, 3246. (b) Mayer, J. M.; Bercaw, J. E. *J. Am. Chem. Soc.* **1982**, *104*, 2157. (c) Evans, W. J.; Meadows, J. H.; Wayda, A. L.; Hunter, W. E.; Atwood, J. L. *J. Am. Chem. Soc.* **1982**, *104*, 2008.

(26) Vitale, A. A.; San Filippo, J. *J. Am. Chem. Soc.* **1982**, *104*, 7341.

(27) (a) Cheney, A. J.; Mann, B. E.; Shaw, B. L.; Slade, R. M. *J. Chem. Soc., Chem. Commun.* **1970**, 1176. (b) Shaw, B. L. *J. Am. Chem. Soc.* **1975**, *97*, 3856.

and although one must also take into account the changes in C–H bond energies on rehybridization it appears that the reaction should be very much enthalpically favored. This indeed is experimentally the case (Table VI), the enthalpy of activation for ring closure of the methylidene being almost half that required for methane loss from the methyl complexes. This dramatic drop in $\Delta H^{\ddagger}$ is, however, almost offset by an equally dramatic increase in the negative value of $\Delta S^{\ddagger}$ to a value close to −30 eu. Without this severe enthalpic inhibition the characterization of the photogenerated methylidene complex would have been difficult. Similar large, negative entropies of activation are characteristic of a number of intramolecular gas-phase organic isomerizations in which highly ordered transition states are believed present.[28] There are three possible contributions to this large increase in entropic inhibition. The first recognizes the fact that the methylidene complex is four coordinate compared to the five-coordinate methyl complexes. Hence, as mentioned above, locking one of the *tert*-butyl groups into effectively a coordination site in the transition state must be more difficult. However, the value of $\Delta S^{\ddagger}$ is still considerably more negative than that found for the four-coordinate $M(OAr')_2(CH_2Ph)_2$ (M = Ti, Zr). Secondly, the interaction of a C–H bond with the π-bond of a methylidene group may require more vigorous geometric constraints than the interaction with a $Ta-CH_3$ σ-bond. The third important difference lies in the fact that activation by methyl groups eventually leads to the formation of a molecule of methane. The partial formation of this extra molecular species may add significantly to the entropy of the transition state compared to the second situation where the methylidene eventually remains tightly bound to the tantalum as a methyl group.

From the above data and discussion it is clear that the idea that intramolecular activation of aliphatic C–H bonds by methylidene functions is more favorable than activation by metal–alkyls has to be examined carefully. The reactivity of the methylidene group over its alkyl counterpart is clearly enthalpically enhanced. However, in the systems we have studied, this enhancement is balanced by a significant entropic inhibition for the intramolecular addition to the tantalum–carbon double bond. These two opposing forces result in there being an isokinetic temperature of 225 °C at which formation of the monocyclometalated complex from either the trimethyl or methylidene complexes is predicted to occur at the same rate. Indeed above this temperature ring closure by loss of methane should be faster than addition to the $Ta=CH_2$ function.

An alternative pathway that we have not considered involves the direct oxidation of the carbon–hydrogen bond to the tantalum center of the methylidene complex. This pathway would seem plausible if one considered the complex **5** to contain a methylene (CH_2) functional group instead of a methylidene (CH_2^{2-}) unit resulting in a formal oxidation state assignment of $+3(d^2)$ instead of $+5(d^0)$ for the tantalum atom. However, there is every indication in the reactivity of related tantalum complexes that the alkylidene assignment best describes the chemistry of this functional group.[7]

Experimental Section

All operations were carried out under a dry nitrogen atmosphere either in a Vacuum Atmospheres dri-lab or by standard Schlenck techniques. Hydrocarbon solvents were dried by distillation from sodium benzophenone under a nitrogen atmosphere. $Ta(OAr')_2Cl_3$ (**1a**) was prepared as previously described.[12] $Ta(OAr'–OMe)_2Cl_3$ (**1b**) was obtained by an identical method with use of Li–OAr'–OMe and recrystallized from hexane. Anal. Calcd for $TaC_{30}H_{46}O_4Cl_3$: C, 47.54; H, 6.11; Cl, 14.03. Found: C, 47.76; H, 6.49; Cl, 15.23.

^1H and ^{13}C NMR spectra were recorded on a Varian Associates XL-200 spectrometer and are referenced to Me_4Si. Probe temperature calibration was performed with ethylene glycol.

Preparation of $Ta(OAr')_2Me_3$ (2a). To an orange solution of $Ta(OAr')_2Cl_3$ (0.50 g) in benzene (25 mL) was added $LiCH_3$ (0.07 g, slight excess). The suspension was stirred until it became colorless, typically 30 min at 25 °C. The solution was filtered and the clear filtrate evaporated in vacuo to leave the product as a white powdery solid. Yield = 0.36 g (78%). Continued exposure to suspended methyl lithium caused the complex to become very dark with the evolution of gas (presumably methane). Anal. Calcd for $TaC_{31}H_{51}O_2$: C, 58.48; H, 8.07. Found: C, 57.90; H, 7.96. Crystals suitable for crystallography were grown from saturated hexane solution by cooling to −15 °C.

$Ta(OAr'–OMe)_2Me_3$ (**2b**) was obtained in an identical fashion with $Ta(OAr'–OMe)_2Cl_3$. Anal. Calcd for $TaC_{33}H_{55}O_4$: C, 56.89; H, 7.95. Found: C, 57.38; H, 8.15.

^1H NMR (C_6D_6, 30 °C): **2a**, δ 1.19 (s, $Ta-CH_3$), 1.45 (s, OC_6H_3-*t*-Bu_2), 6.7–7.2 (m, aromatics); **2b**, δ 1.23 (s, $Ta-CH_3$), 1.45 (s, OC_6H_2-*t*-Bu_2OMe), 3.62 (s, OCH_3), 7.50 (s, C_6H_2). ^{13}C NMR (C_6D_6): **2a**, δ 66.8 ($Ta-CH_3$), 35.3 ($C(CH_3)_3$), 32.2 ($C(CH_3)_3$); **2b**, δ 66.4 ($Ta-CH_3$), 35.8 ($C(CH_3)_3$), 32.4 ($C(CH_3)_3$), 54.8 (OCH_3).

Preparation of $Ta(OC_6H_3$-*t*-$BuCMe_2CH_2)(OAr')Me_2$ (3a). A toluene solution of $Ta(OAr')_2Me_3$ (**2a**) was heated in a closed flask for 24 h at 95 °C. Cooling and removal of solvent under vacuum resulted in essentially quantitative yields of the monocyclometalated complex as a pale powder. Due to its extremely high solubility recrystallization proved impossible. The 4-methoxy derivative **3b** was obtained in an identical manner from $Ta(OAr'–OMe)_2Me_3$ (**2b**).

^1H NMR (C_6D_6, 30 °C): **3a**, δ 1.11 (s, $Ta-CH_3$), 1.38 (s, OC_6H_3-*t*-Bu_2), 1.61 (s, OC_6H-*t*-$BuCMe_2CH_2$), 1.20 (s, OC_6H_3-*t*-$BuCMe_2CH_2$), 2.07 (s, OC_6H_3-*t*-$buCMe_2CH_2$); **3b**, δ 1.17 (s, $Ta-CH_3$); 1.41 (s, OC_6H_2-*t*-Bu_2OMe) 1.68 (s, OC_6H_2OMe-*t*-$BuCMe_2CH_2$), 1.20 (s, OC_6H_2OMe-*t*-$BuCMe_2CH_2$), 2.10 (s, OC_6H_2OMe-*t*-$BuCMe_2CH_2$), 3.48, 3.50 (s, C_6H_2–OMe). ^{13}C NMR (C_6D_6): **3a**, δ 64.5 ($Ta-CH_3$), 94.6 ($Ta-CH_2CMe_2$), 38.05 ($Ta-CH_2CMe_2$), 35.45. ($Ta-CH_2CMe_2$); **3b**, δ 63.8 ($Ta-CH_3$), 98.4 ($Ta-CH_2CMe_2$), 39.0 ($Ta-CH_2CMe_2$), 35.1 ($Ta-CH_2CMe_2$), 54.7, 55.1 (OCH_3).

Preparation of $Ta(OC_6H_3$-*t*-$BuCMe_2CH_2)_2Me$ (4a). Thermolysis of $Ta(OAr')_2Me_3$ (**2a**) or the monocyclometalated complex **3a** in toluene at 124 °C for 24 h in a sealed glass tube resulted in a colorless solution from which the bis-cyclometalated complex could be obtained as a white solid by removal of solvent in vacuo.

^1H NMR (C_6D_6, 30 °C): **4a**, δ 0.91 (s, $Ta-CH_3$), 1.76 (s, OC_6H_3-*t*-Bu), 1.28, 1.35 (s, OC_6H_3-*t*-$BuCMe_2CH_2$), 1.74–1.80 (AB pattern due to OC_6H_3-*t*-$BuCMe_2CH_2$ partly obscured by *t*-Bu signal). ^{13}C NMR (C_6D_6): **4a**, δ 58.5 ($Ta-CH_3$), 95.6 ($Ta-CH_2CMe_2$), 39.5 ($Ta-CH_2CMe_2$), 35.3, 35.5 ($Ta-CH_2CMe_2$).

Preparation of $Ta(OAr')_2(=CH_2)(CH_3)$ (5a). Solutions of the methylidene complex **5a** were generated by photolysis of hydrocarbon solutions (either benzene or hexane) of the complex $Ta(OAr')_2(CH_3)_3$ (**2a**) with use of a 450-W Ace-Hanovia medium-pressure Hg lamp housed in a water-cooled quartz jacket. The solutions were contained in either sealed Pyrex tubes or sealed 5-mm Pyrex NMR tubes for monitoring by ^1H NMR. The solutions were typically maintained at 10 °C during photolysis. Due to the high quantum efficiency of the photoreaction[11,22] essentially complete conversion to the methylidene complex could be achieved in less than 1 h with the sample located between 5 and 10 cm from the lamp source. Due to its facile thermal conversion to the monocyclometalated complex, the methylidene was characterized in solution by NMR methods. The related methylidene complex $Ta(OAr'–OMe)_2(=CH_2)(CH_3)$ (**5b**) was photogenerated by identical procedures from $Ta(OAr'–OMe)_2(CH_3)_3$ (**2b**).

^1H NMR (C_6D_6, 30 °C): **5a**, δ 9.41 (s, $Ta=CH_2$), 1.20 (s, $Ta-CH_3$), 1.47 (s, OC_6H_3-*t*-Bu_2), 6.8–7.1 (m, aromatics); **5b**, δ 9.32 (s, $Ta=CH_2$), 1.33 (s, $Ta-CH_3$), 3.44 (s, OCH_3), 1.50 (s, OC_6H_3-*t*-Bu_2). ^{13}C NMR (C_6D_6): **5a**, δ 236.2 ($Ta=CH_2$), 64.6 ($Ta-CH_3$); **5b**, δ 234.6 ($Ta=CH_2$), 63.7 ($Ta-CH_3$).

Labeling Studies. The complex $Ta(OAr')_2(CD_3)_3$ (**2a**-d_9) was synthesized from $LiCD_3$ (obtained from ICD_3, 99.5% *d*, Merck and Co.) with use of an identical procedure used to obtain the protio complex. Mass spectrometric analysis indicated a parent molecular ion peak at 645 (^{181}Ta; 100% natural abundance), i.e., **2a**-d_9 with the correct ratio of peaks at 646 and 647 for this C_{30} molecule. Thermolysis of this complex to the monocyclometalated complex **3a** followed by analysis showed a parent ion at 626 (**3a**-d_6) with less than 4% of ions with mass 625 (**3a**-d_6). Further thermolysis led to the bis-cyclometalated complex with a base peak at *m/e* 607 (**4a**-d_3) with barely detectable amounts of **4a**-d_2. In contrast the photolysis of $Ta(OAr')_2(CD_3)_3$ to the methylidene complex followed by mild thermolysis led to a monometalated complex with a parent molecular ion peak at 625 (**3a**-d_5) with the peaks at 626 and 627 being consistent with the ^{13}C natural abundance expected for this molecule. Due to the ^{13}C natural abundance peak at 626 it is difficult to accurately determine the amount of **3a**-d_6, but computer simulation studies indicated <5%.

Kinetic Measurements. The two thermal cyclometalation reactions **2a** → **3a** and **3a** → **4a** were monitored kinetically in sealed, evacuated 5-mm NMR tubes in toluene-d_8 solvent. The sealed tubes were thermolyzed

(28) Frost, A. A.; Pearson, R. G. "Kinetics and Mechanism"; John Wiley and Sons: New York, 1961, p 110 and references therein.

by total immersion into a constant-temperature oil bath. The tubes were removed after various amounts of time and cooled in cold water, and the extent of reaction was determined by ^1H NMR. Both the rate constants and activation parameters were determined with use of a linear least-squares fitting procedure. In order to monitor the cyclometalation of the two methylidene complexes **5a,b**, C_6D_6 solutions of the methylidene were first photogenerated in sealed 5-mm NMR tubes. The tubes were then placed in the temperature-controlled probe of a Varian XL200 spectrometer and kinetic data obtained by monitoring the decrease with time of the Ta–CH_2 resonance.

X-ray Diffraction Analysis. Crystal data and data collection parameters are collected in Table I. General operating procedures have been reported previously.[29]

$Ta(OAr')_2Me_3$ (2a). A suitable crystal, cleaved from a larger sample, was characterized by reciprocal lattice search techniques and found to be monoclinic, space group $C2$, Cm, or $C2/m$. Multan 78 was employed in each of the three possible space groups with only $C2$ yielding a solution. A Patterson synthesis as well as the subsequent refinement confirmed the space group. All atoms, including hydrogens, were located and refined. Although the molecular symmetry of the molecule is such that it could possess m symmetry, the final coordinates deviate from those needed for the higher point group. In the final full-matrix least-squares analysis the hydrogen atoms were assigned isotropic thermal parameters, all other atoms being refined anisotropically. A final difference Fourier was featureless with the exception of one peak of 1.24 e/Å^3 located at the tantalum site.

$Ta(OAr'\text{–}OMe)_2Me_3$ (2b). The sample consisted of perfectly formed yellow transparent crystals. A suitable crystal was transferred to the goniostat with use of standard inert atmosphere handling techniques and cooled to −159 °C. A systematic search of a limited hemisphere of reciprocal space located a set of diffraction maxima of orthorhombic symmetry with systematic extinctions corresponding to *Pnma* (or its noncentric equivalent). Solution and refinement of the structure were possible in the centric setting.

Due to air conditioning failure, the crystal was lost before data collection was complete, and 46 reflections in the $0k1$ zone were not recorded. It was decided that the lack of these data would not cause any systematic errors, so no attempt was made to recollect on a new crystal. All hydrogen atoms were located and refined isotropically with anisotropic thermal parameters for the non-hydrogen atoms.

A final difference Fourier was featureless, the largest peak being 0.72 e/Å^3. No absorption correction was made.

Acknowledgment. We thank the National Science Foundation (Grant CHE-8219206 to I.P.R.) for support of this research.

Supplementary Material Available: Tables of fractional coordinates of hydrogen atoms, anisotropic thermal parameters, complete bond distances and angles, and observed and calculated structure factors (39 pages). Ordering information is given on any current masthead page.

(29) Huffman, J. C.; Lewis, L. N.; Caulton, K. G. *Inorg. Chem.* **1980**, *19*, 2755.

An Unusual Trimetallic Cluster and Its Hypothetical Solid-State Counterparts

Marjanne C. Zonnevylle, Jérôme Silvestre, and Roald Hoffmann*

Contribution from the Department of Chemistry and Materials Sciences Center, Cornell University, Ithaca, New York 14853. *Received September 16, 1985*

Abstract: The electronic structure of the $Cp_2Co_3(CO)_4^{2-}$ core of the recently synthesized $Cp_3Co_3(CO)_4(YbCp_2)_2$ molecule is analyzed by a fragment orbital molecular orbital analysis. The odd electron in this unusual linear trinuclear complex should occupy a metal and Cp based orbital of special symmetry. Reduction may lead to Co–Co bond lengthening and a tetrahedral geometry at the central Co. The relationship to $Fe_3(CO)_{11}^{2-}$ and allene is traced. The series $CpCo(CO)_2$, $Cp_2Co_2(CO)_2$, and $Cp_2Co_3(CO)_4^{2-}$ leads us to think of several alternative and as yet unsynthesized $Co(CO)_2$ polymers.

Among the multitude of trimetalic clusters known today, few of those built upon a metal–metal bonded framework abandon the triangular geometry typified by the series $M_3(CO)_{12}$, M = Fe, Ru, Os[1a–c] (**1**). An early known example of such a dissenter is Dahl's $Fe_3S_2(CO)_9$ (**2**), which features only two Fe–Fe bonds.[2] The backbone angle α, that is, the angle between the two metal–metal bonds, is only 81.0°. The complex is still best described as triangular, albeit open triangular. Its desire to keep one bond

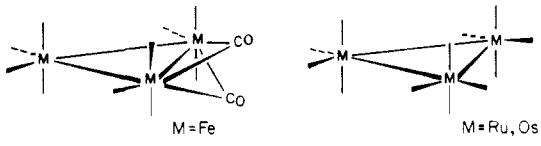

1

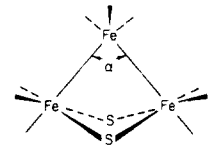

2

long is easily understood within the framework of skeletal electron pair counting schemes such as those of Wade and Mingos.

Moving toward a more linear geometry, we find $Fe_3(CO)_{11}[Cp^*_2Yb]_2$ (where $Cp^* = C_5Me_5$) which also has two Fe–Fe bonds, but the backbone angle is now opened[3] to ~162°, as depicted in **3**. We shall return to this complex shortly. For now, suffice it to notice that the $Fe_3(CO)_{11}^{2-}$ core, **3**, carries four bridging and seven terminal carbonyl groups. Of the latter, six are symmetrically distributed on the two end-iron atoms. The seventh one is located on top of the central Fe atom, at the apex

(1) (a) Cotton, F. A.; Troup, J. M. *J. Am. Chem. Soc.* **1974**, *96*, 4155. (b) Mason, R.; Rae, A. I. B. *J. Chem. Soc. A.* **1968**, 778. (c) Corey, E. R.; Dahl, L. F. *Inorg. Chem.* **1962**, *1*, 521.

(2) Wei, C. H.; Dahl, L. F. *Inorg. Chem.* **1965**, *4*, 493. See also Bard, A. J.; Cowley, A. H.; Leland, J. K.; Thomas, J. N.; Norman, N. C.; Jutzi, P.; Morley, C. P.; Schlüter, E. *J. Chem. Soc., Dalton Trans.* **1985**, 1303.

(3) Tilley, T. D.; Andersen, R. A. *J. Am. Chem. Soc.* **1982**, *104*, 1772.

0002-7863/86/1508-1509$01.50/0